Quantum information analysis of the phase diagram of the half-filled extended Hubbard model

C. Mund,[1] Ö. Legeza,[2] and R. M. Noack[1]
[1]*Fachbereich Physik, Philipps-Universität Marburg, 35032 Marburg, Germany*
[2]*Research Institute for Solid State Physics and Optics, P.O. Box 49, H-1525 Budapest, Hungary*
(Received 29 April 2009; published 25 June 2009)

We examine the phase diagram of the half-filled one-dimensional extended Hubbard model using quantum information entropies within the density-matrix renormalization group. It is well known that there is a charge-density-wave phase at large nearest-neighbor and a small on-site Coulomb repulsion and a spin-density wave at small nearest-neighbor and large on-site Coulomb repulsion. At intermediate Coulomb interaction strength, we find an additional narrow region of a bond-order phase between these two phases. The phase transition line for the transition out of the charge-density-wave phase changes from first order at strong coupling to second order in a parameter regime where all three phases are present. We present evidence that the additional phase-transition line between the spin-density-wave and bond-order phases is infinite order. While these results are in agreement with recent numerical work, our study provides an independent unbiased means of determining the phase boundaries by using quantum information analysis, yields values for the location of some of the phase boundaries that differ from those previously found, and provides insight into the limitations of numerical methods in determining phase boundaries, especially those of infinite-order transitions.

DOI: 10.1103/PhysRevB.79.245130 PACS number(s): 71.10.Fd, 71.10.Hf, 71.30.+h

I. INTRODUCTION

The one-dimensional Hubbard model is one of the earliest and most-studied models of strongly correlated itinerant electrons.[1] Its phase diagram at half filling was one of the first treated using quantum Monte Carlo for quantum lattice systems,[2] one of the first modern numerical methods for these systems. Thus, it is perhaps surprising that the details of the phase diagram of this model at half filling have only recently been established.[3–5]

In this work, we determine the ground-state phase boundaries for the half-filled system using methods based on quantum information[6–11] calculated using the density-matrix renormalization group (DMRG).[12–14] These methods have a number of advantages over other methods involving gaps, correlation functions, or order parameters.[11,15] First, they involve only the properties of the ground state (or, in practice, a numerical approximation to the true ground state) and so can be calculated easily and accurately. Second, the behavior of the various quantum information entropies can be directly related to quantum critical behavior, so that they provide unbiased indicators of quantum phase transitions.[6–9] Finally, they are quantities both intimately related to the fundamental approximation of the DMRG and easily and naturally calculated within the DMRG algorithm.[16,17] Comparison with results from other indicators of quantum phase transitions lends insight into the accuracy and limitations of both the indicators and the underlying numerical method.

The one-dimensional extended Hubbard model (EHM) (Ref. 18) is a relatively simple model which describes hopping of spin-$\frac{1}{2}$ fermions between neighboring sites on a lattice. The fermions interact with each other through on-site and nearest-neighbor (NN) interactions, as described by the Hamiltonian

$$H = -t\sum_{i=1,\sigma}^{N-1}(c_{i\sigma}^{\dagger}c_{i+1\sigma} + c_{i+1\sigma}^{\dagger}c_{i\sigma}) + U\sum_{i=1}^{N} n_{i\uparrow}n_{i\downarrow} + V\sum_{i=1}^{N-1} n_i n_{i+1}. \quad (1)$$

Here $c_{i\sigma}^{\dagger}(c_{i\sigma})$ creates (annihilates) an electron with spin σ on site i, $n_{i\sigma}=c_{i\sigma}^{\dagger}c_{i\sigma}$, and $n_i=n_{i\uparrow}+n_{i\downarrow}$. The parameter t denotes the strength of the intersite hopping, U denotes the strength of the on-site interaction, and V denotes the strength of the nearest-neighbor interaction. Since the nearest-neighbor and on-site interactions originate from the (repulsive) Coulomb potential in most materials, we consider only $U,V>0$ in this work. In general, we will consider finite lattices of size N with open boundary conditions.

Although the model is relatively simple, the phase diagram of the half-filled system is more complicated than one might expect. When $V=0$, the EHM reduces to the one-dimensional Hubbard model which is exactly solvable using the Bethe ansatz.[19] From this exact solution, it is known that the system is in a spin-density-wave (SDW) phase for all $U>0$. This picture is reinforced by the effective model for strong coupling ($U/t\gg 1$), the Heisenberg model, which has a SDW ground state for antiferromagnetic spin exchange. One expects the SDW phase to remain the ground state for finite V, as long as $U/V\gg 1$. In the opposite limit $V/U\gg 1$, one expects the system to form a commensurate charge-density wave (CDW) with an alternating spontaneously broken symmetry, i.e., sites with average occupation $\langle n_i\rangle>1$ alternate with sites with $\langle n_i\rangle<1$. Such a picture is obtained both in a strong-coupling perturbation theory[20] and in a weak-coupling renormalization group treatment (g-ology).[21] In fact, the phase boundary between these two phases is predicted to be at $U=2V$, to lowest order, by both treatments.

While a phase diagram containing only these two phases

would not be particularly interesting in and of itself, a prediction that a bond-order-wave (BOW) phase, a phase characterized by a spontaneously broken symmetry in which strong and weak bonds alternate, occurs near the CDW-SDW phase boundary at (approximately) $U=2V$ for intermediate coupling[22] has sparked new interest in the phase diagram. In addition, g-ology predicts the CDW-SDW phase transition to be continuous, while strong-coupling theory predicts it to be first order, i.e., discontinuous. As a result, a number of papers on this issue have been published in the last few years, some containing contradictory results.[3–5,23] Apparent agreement in the numerically determined ground-state phase diagram is present in two recent treatments.[3,5] However, in both of these calculations, the same quantities, the spin and charge exponents, the bond order parameter, and the spin and charge gaps are used to determine the phase boundaries, and in the latter one consistency checks or realistic error estimates are not present. In view of the fact that both underlying numerical methods, quantum Monte Carlo (QMC) and the DMRG yield results that are numerically exact for this system, it is not surprising that the subsequent similar analyses of the data yield essentially the same results. As we shall see, alternative ways of determining the phase boundaries yield more deviation than is indicated by this agreement.

In recent years, various types of quantum entropies have proven themselves to be a useful and accurate tool for determining the nature and critical parameter values of quantum phase transitions (QPTs).[7–11,15,24–26] Our goal is to combine these newly developed methods with accurate numerical calculations to independently determine the phase diagram.

In this paper, we calculate the one-site, two-site, and block entropies of the EHM using the DMRG and use these quantities to determine the nature and location of the phase boundaries in its phase diagram. The remainder of this paper is organized as follows. The concepts and methods used in our calculation are discussed in Sec. II, with Sec. II A defining the one-site, two-site, and block entropies and Sec. II B describing the DMRG method used. Results for these quantities calculated using the DMRG are presented in Sec. III. Section III C explores the limitations of using quantities such as order parameters to determine phase boundaries. Finally, the implications of our results as well as a comparison with previous work are contained in Sec. IV.

II. CONCEPTS AND METHODS

A. Quantum entropy

Wu *et al.*[25] argued that, quite generally, QPTs are signaled by a discontinuity in some measures of entanglement in the quantum system. One such measure is the concurrence,[24] which has been utilized by a number of authors[8–10,27–31] in their studies of spin models. The local measure of entanglement (the one-site entropy)[32] has been proposed by Zanardi[6] and Gu *et al.*[7] or the negativity by Vidal and Werner[33] to identify QPTs. All of these quantities exhibit anomalies, i.e., either discontinuities in the quantity itself or in its higher derivatives or extrema, at points in parameter space that correspond to QPTs in exactly solvable models. What kind of anomaly occurs depends on the quantity and on the type of QPT; sometimes the anomaly appears only in some but not all of the quantum information entropies.[11] However, it has become clear from recent work[7,15] that, when the appropriate variant of the quantum information entropy is chosen, it can be used as a particularly convenient and accurate probe of the QPT. One example of this is the two-site entropy, a good probe of transitions to dimerized phases such as the BOW phase we study here.[11]

All of the quantum entropies discussed here have as their starting point the reduced density matrix of a bipartite system. Assuming that a quantum mechanical system in a pure state $|\Psi\rangle$ is divided into two parts, part A with complete orthonormal basis $|i\rangle$ and part B with complete orthonormal basis $|j\rangle$, the wave function can be expressed as

$$|\Psi\rangle = \sum_{i,j} C_{ij}|i\rangle \otimes |j\rangle. \tag{2}$$

The density matrix of the entire system is defined as

$$\rho = |\Psi\rangle\langle\Psi| \tag{3}$$

and the reduced density matrix for subsystem A is

$$\rho_A = \mathrm{tr}_B(|\Psi\rangle\langle\Psi|), \tag{4a}$$

$$= \sum_j \langle j|\Psi\rangle\langle\Psi|j\rangle, \tag{4b}$$

$$= \sum_{i,i',j} C_{ij}C^*_{i'j}|i\rangle\langle i'|. \tag{4c}$$

The von Neumann entropy for subsystem A is then

$$S_A = -\mathrm{Tr}\ \rho_A \ln \rho_A = -\sum_\alpha \rho_\alpha \ln(\rho_\alpha), \tag{5}$$

where ρ_α are the eigenvalues of the density matrix ρ_A. It is also useful to define the density matrix in terms of a (unnormalized) projector which takes subsystem A from state $|i'\rangle$ to state $|i\rangle$,

$$\langle i|\rho_A|i'\rangle \equiv \langle\Psi|P_{i',i}|\Psi\rangle = \langle\Psi|\left(\sum_j |i\rangle \otimes |j\rangle\langle j| \otimes \langle i'|\right)|\Psi\rangle. \tag{6}$$

For simple subsystems and an appropriate choice of basis $|i\rangle$, the operator $P_{i',i}$ can be expressed in terms of relatively simple operators, so that its matrix elements can be directly calculated using the corresponding observables;[34] this will be used in the following.

1. One-site entropy

In order to form the one-site entropy, which we will denote $S_\ell(1)$, the subsystem A is simply taken to be a particular single site ℓ. Since Hamiltonian (1) contains no spin-flip process, the reduced density matrix can be obtained directly in diagonal form if we take the spin occupation basis $(|0\rangle, |\uparrow\rangle, |\downarrow\rangle, |\uparrow\downarrow\rangle)$ as the basis states $|i\rangle$ in Eq. (6). In this basis, we can directly obtain the eigenvalues from the expectation values of the four operators[34]

$$\langle\uparrow\downarrow|\rho_\ell|\uparrow\downarrow\rangle = \langle n_{\ell\uparrow}n_{\ell\downarrow}\rangle,$$

$$\langle\downarrow|\rho_\ell|\downarrow\rangle = \langle(1-n_{\ell\uparrow})n_{\ell\downarrow}\rangle,$$

$$\langle\uparrow|\rho_\ell|\uparrow\rangle = \langle n_{\ell\uparrow}(1-n_{\ell\downarrow})\rangle,$$

$$\langle 0|\rho_\ell|0\rangle = \langle(1-n_{\ell\uparrow})(1-n_{\ell\downarrow})\rangle.$$

The one-site entropy is relatively easy to calculate because it requires only four local measurements on site ℓ. While the one-site entropy is useful in some cases for characterizing first-order QPTs, it is typically not well suited for determining higher order QPTs because anomalies are often only discernible for large system sizes and are sometimes not present at all.[7,11] In particular, changes in intersite bond strength have no influence on it. Since the one-site entropy necessarily only depends on quantities that are localized on that one site (in fact, only on the average occupancy and on the average double occupancy), it cannot contain spatial information that is nonlocal.

2. Two-site entropy

It is therefore often useful to examine the von Neumann entropy associated with a larger subsystem. One convenient choice of subsystem A is that of two sites p and q, i.e., the two-site entropy $S_{p,q}$. In particular, we are interested in characterizing a BOW phase, which, for open boundary conditions, will have a broken bond-centered spatial symmetry. Thus, we are principally interested in the behavior of the two-site entropy for different bonds, i.e., we take p and q to be pairs of nearest-neighbor sites. Therefore, the two-site entropy will be denoted as $S_p(2)$ in this paper, meaning $S_{p,p+1}$.

The two-site entropy can be obtained by calculating and diagonalizing the reduced density matrix for the two sites. As for the one-site density matrix, its matrix elements in the occupation number basis can be expressed straightforwardly in terms of expectation values localized to the two sites by considering the projector of Eq. (6). However, the result is necessarily somewhat more complicated than for the one-site density matrix. Since spin and particle number are conserved quantum numbers in Hamiltonian (1), the resulting reduced density matrix is block diagonal (rather than diagonal as for the one-site case) and has 26 independent matrix elements (for details, see Ref. 34). Hence, 26 independent measurements followed by the appropriate matrix diagonalization and the summation of Eq. (5) must be performed for every two-site entropy calculated.

Note that calculating all $N(N-1)$ two-site entropies would be prohibitively expensive for large system sizes. While considering only nearest-neighbor bonds reduces this to $N-1$, it is usually sufficient to calculate the entropies of the two pairs of innermost sites $S_{N/2-1}(2)$ and $S_{N/2}(2)$, i.e., two bonds chosen to be in the middle of the system to minimize boundary effects, to characterize a BOW phase.

3. Block entropy

The block entropy is also based on splitting the system into two subsystems A and B. However, subsystem A is now taken to contain the ℓ contiguous sites 1 to ℓ and subsystem B to contain the remainder, sites $\ell+1$ to N. (Note that other choices of sets of contiguous sites are also possible.) We then calculate the von Neumann entropy $S(\ell)$ using Eq. (5) for $\ell \in 1,\ldots,N$. Note that calculating the projector $P_{i',i}$ of Eq. (6) would be prohibitively complicated and expensive. Here, we instead calculate the density matrix directly from the wave function using Eq. (4c). Fortunately, the wave function for all divisions of the system ℓ is readily available in the appropriate finite-system step of the DMRG algorithm, and, in fact, the corresponding von Neumann entropy is intimately related to the approximation made in the DMRG.[16,17]

Unlike the two-site entropy, which has an finite upper bound (ln 16 for Hubbard-type models), the block entropy generally grows as $\mathcal{O}(\ln N)$ for critical one-dimensional systems[35] (but scales to a finite value for noncritical systems). Although such a potential divergence would at first glance seem favorable for studying QPTs, the situation is actually more complicated: boundary effects from open boundary conditions should have a stronger influence on the block entropy than on a more locally defined quantity such as the one-site or two-site entropy. It is therefore not clear which of these entropies can more accurately detect QPTs, but it seems sensible to expect that fast growing peaks are better detected by the block entropy, while nondiverging anomalies such as discontinuities in derivatives, can be more precisely determined by the two-site entropy.

B. DMRG

The DMRG calculations were carried out using the finite-system algorithm[12–14] on systems with (mostly) open boundary conditions with from $N=32$ to $N=512$ lattice sites. Open rather than periodic boundary conditions were used for two reasons: first, the DMRG is substantially more accurate for fixed system size and the computational effort is significantly smaller. Second, since open boundary conditions explicitly break the translational invariance, a corresponding spontaneously broken symmetry of the ground state, which, strictly speaking, can only occur in the thermodynamic limit, appears in the entropy profiles of finite-sized systems.[15,36] This is, for example, the case for the BOW phase.

Since only ground-state properties are required to calculate the von Neumann entropies, we only need to calculate the ground-state wave function and the appropriate observables for the half-filled system. We have used dynamic block-state selection, which chooses the size of the Hilbert space retained in each truncation by keeping the block entropy of the discarded density-matrix eigenstates constant.[17] It is important to do this because the accuracy of the von Neumann entropy as calculated using the approximate DMRG wave function in Eq. (4c) is directly related to the entropy threshold used. In our calculations we used a threshold for the quantum information loss[17] of $\chi<10^{-10}$, which yields extremely precise results and requires a maximum of approximately $m=3000$ block states to be retained. In general, we estimate that the errors due to the truncation in the DMRG calculations are negligible in comparison to the uncertainties arising from the finite-size scaling.

C. Limitations of other quantities

Naively, the most straightforward way to determine the existence and extent of a BOW phase would probably be to

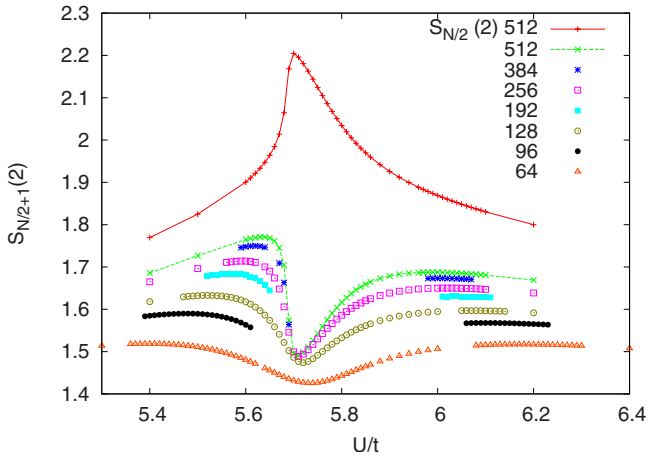

FIG. 1. (Color online) Two-site entropy $S_{N/2+1}(2)$ for $V/t=3$ plotted as a function of U/t. System sizes range from $N=64$ to $N=512$ sites.

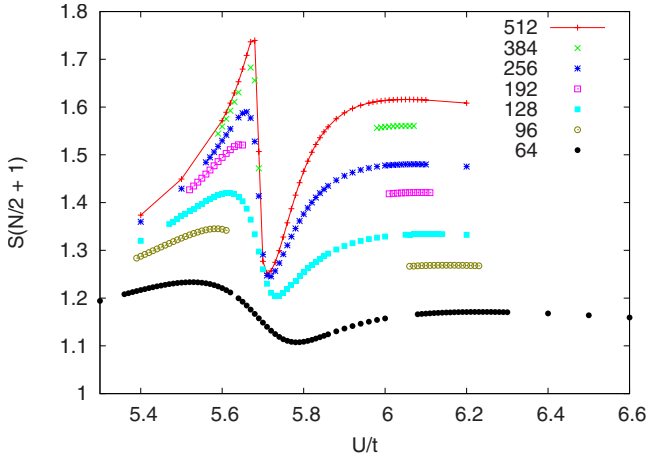

FIG. 2. (Color online) Block entropy at the center of the chain $S(N/2+1)$ for $V/t=3$ and system sizes from $N=64$ to $N=512$ sites.

examine the bond order parameter defined as

$$B = \frac{1}{N}\sum_{i=1,\sigma}^{N-1} (-1)^i \langle c_{i+1\sigma}^{\dagger} c_{i\sigma} + c_{i\sigma}^{\dagger} c_{i+1\sigma} \rangle. \tag{7}$$

Whether the bond order parameter is finite or vanishing in the thermodynamic limit would determine whether a given point in parameter space is ordered or not, and a grid of such points can be used to determine the phase boundaries.

Unfortunately, there are two major problems with this strategy. First, the transition between the BOW and SDW phases is expected to be infinite order, and we indeed find behavior characteristic of an infinite-order transition. This means that the extrapolated bond order parameter tends to zero exponentially as the BOW-to-SDW transition is approached. Second, while it is known that the bond order parameter is linear in $1/N$ in the CDW phase, where N is the system size, and proportional to $1/\sqrt{N}$ in the SDW phase, the analytic form of the finite-size scaling in the BOW phase is not known and changes nature as the transition is approached. We will examine this issue in more detail in Sec. III C.

Unfortunately, similar difficulties arise in other quantities that are typically used to determine critical parameters. In particular, the charge gap goes to zero in a clear manner at the CDW-BOW phase transition but does not exhibit any anomalies at the BOW-SDW transition. The spin gap, on the other hand, does go to zero at the BOW-SDW transition, but, like the bond order parameter, with an exponential dependence. Therefore, it is also not well suited for exactly determining the phase boundary.

III. RESULTS

We consider first the behavior of the two-site and block entropies. In order to map out the phase boundaries, we have swept V from $V=2$ to $V=5.5$ in steps of 0.5 for a number of values of U. For all sweeps, we find that two peaks develop in both the two-site entropy (Fig. 1) and in the block entropy (Fig. 2) for sufficiently large systems. Note that the second peak in the block entropy can only be seen at system sizes of $N=96$ and larger. This slow size dependence might be the reason why this phase was not seen by Deng and co-workers.[7]

We interpret the peak at lower U as marking the CDW-BOW phase transition at the corresponding system size and the peak at larger U as indicating the BOW-SDW phase transition. The differing shapes of the two peaks are consistent with the picture that the CDW-BOW transition is first order in this parameter regime,[3] while the BOW-SDW transition shows characteristics of an infinite-order transition.

The interpretation that the intervening phase is a BOW phase is supported by the behavior of the two-site entropy for two adjacent (odd and even) bonds in the center of the lattice plotted for the largest system size $N=512$ in Fig. 1. The dimerization entropy is given by $D_s=S_{N/2+1}(2)-S_{N/2}(2)$, which is the difference between the two $N=512$ curves. It is clear that this difference reaches a marked maximum between the two peaks associated with the phase transitions. Finite-size extrapolation (not shown) indicates that D_s remains finite in the thermodynamic limit in the intermediate phase.

The positions of the two peaks in the two site or block entropy can then be extrapolated to the thermodynamic limit. While the functional form of this extrapolation is not exactly known, using a fourth-order polynomial yields stable results, with a rapid falloff in coefficient size for higher orders. Therefore, the behavior is predominantly linear. This can be seen in Fig. 3.

A. CDW-BOW transition

A comparison of Figs. 1 and 2 clearly shows that the peaks in the block entropy at lower U are sharper and higher than those in the two-site entropy. In addition, the position of the peaks in the block entropy matches the jump in the one-site entropy (see Fig. 4) better than the position of the peak in the two-site entropy. Therefore, we conclude that the block entropy is, in general, a better indicator of the position of the CDW-BOW transition than the two-site entropy. As

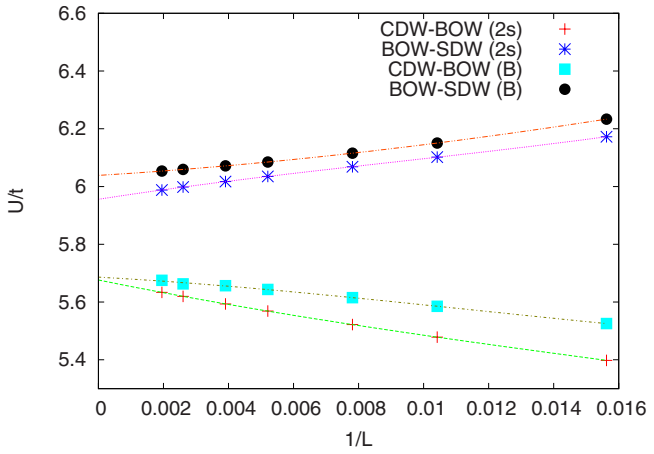

FIG. 3. (Color online) Finite-size extrapolation of the peaks in Figs. 1 and 2 to the thermodynamic limit $1/L \to 0$, using fourth-order polynomials in $1/L$. "$2s$" labels the two-site entropy and "B" labels the block entropy.

can be seen in Fig. 3, the fits to the two-site and the block entropies (the two lower curves) match almost exactly in the thermodynamic limit, so that this issue is virtually irrelevant here.

A more difficult issue is to determine where nature of the CDW-BOW transition changes from first-order to continuous. This can best be investigated using the finite-size extrapolation of the one-site entropy. In Fig. 4, we show the one-site entropy extrapolated to the thermodynamic limit using a polynomial of cubic order. It is apparent that the entropy has a jump at the transition point when $V/t \geq 4$, a clear indication of a first-order transition. At approximately $V/t = 3$, the transition is close to becoming continuous in that a jump is no longer present. For smaller values of V/t (not shown), it is clearly continuous. Therefore, we conclude that the first-order-to-continuous bicritical point must occur somewhere near, but below $V=3$. Note that it is difficult to determine the location of this point with more accuracy because one would have to determine whether or not an increasingly small jump is present in the finite-size extrapolated data as the bicritical point is approached on a sufficiently finite grid.

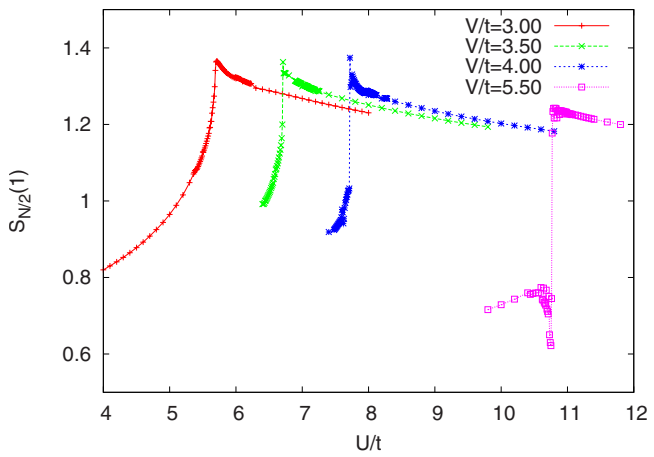

FIG. 4. (Color online) Extrapolated one-site entropy $S_{N/2}(1)$ plotted as a function of U/t for various values of V/t.

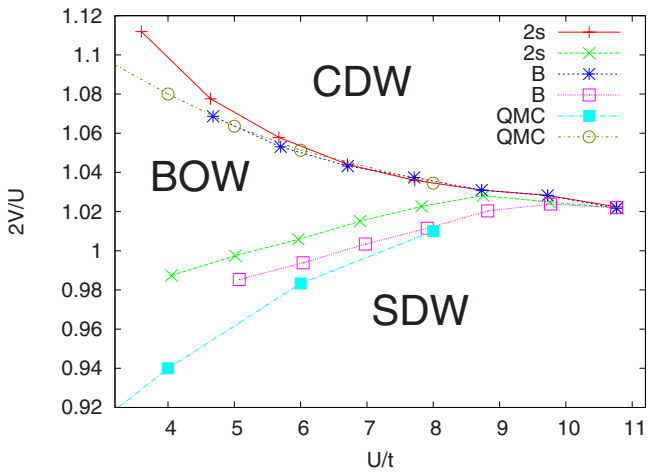

FIG. 5. (Color online) The phase diagram in the tilted U-V plane, showing phase boundaries determined using the two-site entropy ($2s$), the block entropy (B), and including results from Ref. 3, determined from QMC calculations.

B. BOW-SDW transition

The BOW-SDW transition is believed to be infinite order[18] and is therefore much harder to characterize. While we were able to obtain a fairly good estimate for the position of the CDW-BOW transition just by examining the bond order parameter, this is not possible for the BOW-SDW transition, as discussed in Sec. III C. As can be seen in Figs. 1 and 2, the maxima for the BOW-SDW transition (the peaks at higher U/t) are much broader. Therefore, small errors in the numerical calculations would have a bigger influence on the result than for the case of the CDW-BOW transition. Due to this, we have carried out very high-precision calculations, as already described in Sec. II B.

Results for the phase boundaries are shown in Fig. 5 plotted in the tilted V-U phase, i.e., with axes $2V/U$ and U, so that the transition region is discernible. Included are data from Ref. 3, in which the phase boundaries were determined from the spin and charge exponents calculated using QMC methods. There is generally very good agreement for the location of the CDW-BOW transition, with some deviations of the results from the two-site entropy at smaller U/t values. As we have argued above, the block entropy is a better indicator of the position of this transition because the peak is better developed and grows more rapidly with system size.

For the BOW-SDW transition, the two-site and the block entropies coincide perfectly upon scaling for higher U and V values, where only a first-order transition is present, as can be seen in Fig. 5. However, there is a discrepancy in the position of the peaks in the infinite-system extrapolations of the two-site and the block entropies (see Fig. 3) for smaller values of U and V. This occurs for the entire range of parameter values in which a BOW phase and, therefore, an infinite-order transition is present. This is probably partially due to uncertainty in localizing the broad peak in the entropies corresponding to the BOW-SDW transition. In addition, due to the strong increase in the block entropy with system size below $U/t \approx 4$, we cannot treat systems of more than a few hundred lattice sites for fixed $\chi = 10^{-10}$, leading to in-

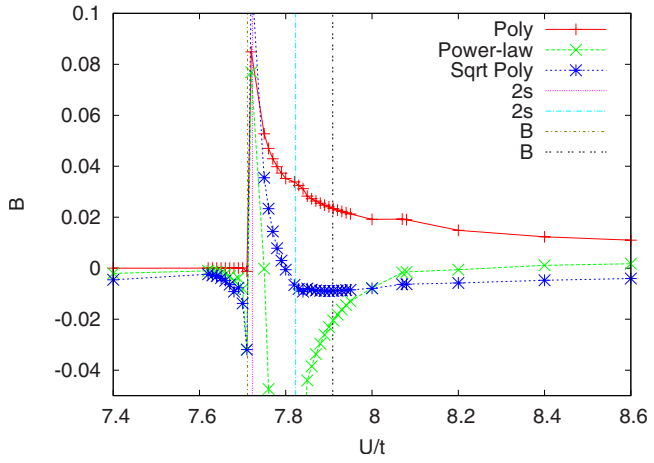

FIG. 6. (Color online) Bond order parameter B for $V/t=4$ extrapolated to the thermodynamic limit using fits to three different functions: fit to a third-order polynomial in $1/N$ (poly), fit to a third-order polynomial in $1/\sqrt{N}$ (sqrt-poly), and fit to a power law $1/N^{\alpha}$ (power law) with α a fitting parameter plotted as a function of U/t. The vertical lines indicate the transition point determined using the two-site entropy ($2s$) and the block entropy (B).

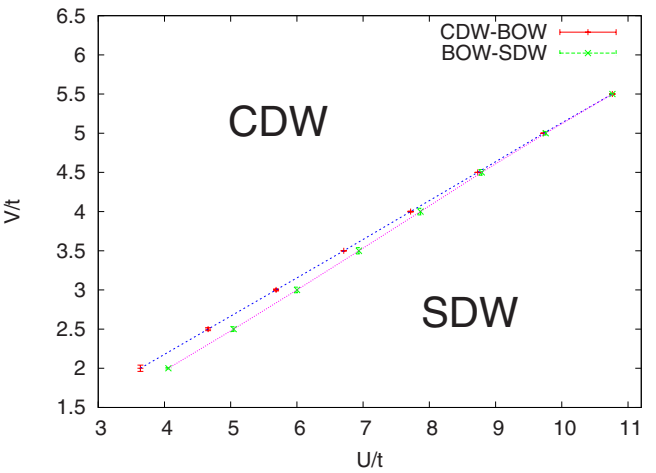

FIG. 7. (Color online) The phase diagram in the U-V plane obtained from our calculations. On this scale, uncertainties in the position of the transition lines are smaller or about the size of the symbols. The phase in the narrow region between the two transition lines is BOW.

creased uncertainty in the finite-size extrapolation. For $U/t<3$, the second peak in the entropy functions develop only for $N\geq 96$, quite severely limiting the extrapolation to infinite system size. We therefore display the phase diagram only for $U/t>3$ in Fig. 5

C. Bond-order-parameter results

As already mentioned in Sec. II C, we have carried out calculations for the bond order parameter to very high precision. The resulting data are sufficiently accurate so that they can be regarded as essentially exact for a particular size for fitting purposes. We have carried out the extrapolation to the infinite-system limit by fitting to three different functions: a polynomial in $1/N$, a polynomial in $1/\sqrt{N}$, and a power law of the form $1/N^{\alpha}$. The extrapolated data are shown in Fig. 6. In the CDW phase, to the left of the transition indicated by vertical lines, the fit to a polynomial in $1/N$ gives the best result, yielding the expected value (zero) to the best accuracy. In the SDW phase, for $U/t\gtrsim 8$, the polynomial fit in $1/\sqrt{N}$ and the fit to a power law work better, yielding the expected value of zero within reasonable accuracy. This is indicative of a scaling whose dominant term falls off more slowly than $1/N$. In the intermediate region, i.e., in the BOW phase, the results differ significantly, with both the fit to powers of $1/\sqrt{N}$ and the power-law fit extrapolating to spurious negative values. In addition, the power-law fit is clearly unstable in the BOW region. While the fit to a polynomial in $1/N$ seems to be more stable, it clearly overestimates the bond order parameter significantly in both the SDW phase and in most of the BOW region.

Therefore, we conclude that the behavior of the bond order parameter can be used to confirm the position of the CDW-BOW phase transition but is notoriously unreliable for determining the location of the BOW-SDW phase transition.

IV. PHASE DIAGRAM AND DISCUSSION

We now summarize the current state of knowledge of the phase diagram of the half-filled extended Hubbard model and discuss open issues and uncertainties. The overall phase diagram is relatively well understood; our results are depicted in Fig. 7. The presence of the SDW phase at $U\ll 2V$ and the CDW phase at $U\gg 2V$ have been long understood, as well as the fact that the transition occurs at $U\approx 2V$. The picture of there being a single first-order transition line at strong U and V (Ref. 20) is also well established. Our work lends support to a picture in which an intermediate BOW phase is present between the CDW and SDW phases for intermediate to small U and V; our results indicate that this phase is present for $V/t\lesssim 5$. At this point, we find that the first-order CDW-SDW transition line bifurcates into a first-order CDW-BOW transition line and an infinite-order BOW-SDW transition line. The CDW-BOW transition line remains first-order at a bicritical point at somewhat smaller V/t, below which it becomes continuous, presumably second order. These results are in reasonable agreement with the results of Refs. 3 and 5. We therefore regard these features of the phase diagram as being well established.

We now discuss details of the phase transition more quantitatively. As we have seen in Fig. 5, there is not much uncertainty in the position of the CDW-BOW phase transition. The remaining interesting question for this transition is the location of the bicritical point, i.e., exactly where the phase-transition line goes from being first order to being continuous (presumably second order). However, as we have pointed out in Sec. III A, entropy measurements can only roughly determine that this point occurs at around $V/t=3$ and are not an ideal measurement to locate it more accurately. While other authors have obtained putatively more accurate values for the location of this bicritical point,[3,5] we point out that the inaccuracies in our method reflect intrinsic limitations of the numerical methods, which stem both from the DMRG truncation error as well as from the limitations of working with finite systems.

The exact position of the BOW-SDW phase-transition line is also somewhat uncertain. There is a small but significant discrepancy in our calculations between the values obtained from the two-site entropy and those obtained from the block entropy; however, both of these extrapolated values seem to converge smoothly to the same line at the tricritical point. The most likely explanation for the discrepancy in the extrapolations lies in the finite-size extrapolation, i.e., more precise results could be obtained if larger system sizes could be treated. The deviations between the two values for the transition line can be taken as a rough estimate of the uncertainty in the position of the line. In addition, both of these values deviate from those of Refs. 3 and 5 (see Fig. 5), a deviation to larger values of V, i.e., to a narrower BOW phase, in both cases.

In summary, the DMRG method coupled with the use of single-site, two-site, and block entropies, is a powerful relatively unbiased method to determine subtle properties of phase diagrams such as that of the extended Hubbard model at half filling. However, the limitations of the numerical results reflect the intrinsic limitations of the method and the problem studied. In particular, three aspects of the phase diagram studied here remain difficult to pin down numerically: the exact position at which the CDW-SDW line bifurcates into CDW-BOW and BOW-CDW transition lines, the position of the bicritical point at which the CDW-BOW transition goes from first to second order, and the exact position of the infinite-order BOW-SDW transition. In addition, our calculations make clear that quantitative determination of the transition lines becomes very difficult in the region of small U and V.

ACKNOWLEDGMENTS

The authors thank A. Sandvik for providing data from Ref. 3 in numerical form and F. Gebhard for helpful discussions. This research was supported in part by the Hungarian Research Fund (OTKA) under Grants No. K 68340 and No. K 73455, and by the János Bolyai Research Fund.

[1] J. Hubbard, Proc. R. Soc. London, Ser. A **276**, 238 (1963).
[2] J. E. Hirsch, R. L. Sugar, D. J. Scalapino, and R. Blankenbecler, Phys. Rev. B **26**, 5033 (1982).
[3] A. W. Sandvik, L. Balents, and D. K. Campbell, Phys. Rev. Lett. **92**, 236401 (2004).
[4] E. Jeckelmann, Phys. Rev. Lett. **89**, 236401 (2002).
[5] S. Ejima and S. Nishimoto, Phys. Rev. Lett. **99**, 216403 (2007).
[6] P. Zanardi, Phys. Rev. A **65**, 042101 (2002).
[7] S.-J. Gu, S.-S. Deng, Y.-Q. Li, and H.-Q. Lin, Phys. Rev. Lett. **93**, 086402 (2004).
[8] J. Vidal, G. Palacios, and R. Mosseri, Phys. Rev. A **69**, 022107 (2004).
[9] J. Vidal, R. Mosseri, and J. Dukelsky, Phys. Rev. A **69**, 054101 (2004).
[10] M.-F. Yang, Phys. Rev. A **71**, 030302(R) (2005).
[11] O. Legeza and J. Sólyom, Phys. Rev. Lett. **96**, 116401 (2006).
[12] S. R. White, Phys. Rev. Lett. **69**, 2863 (1992).
[13] S. R. White, Phys. Rev. B **48**, 10345 (1993).
[14] R. M. Noack and S. R. Manmana, in *Diagonalization- and Numerical Renormalization-Group-Based Methods for Interacting Quantum Systems*, edited by A. Avella and F. Mancini, AIP Conference Proceeding No. 789 (AIP, New York, 2005), pp. 93–163.
[15] O. Legeza, J. Sólyom, L. Tincani, and R. M. Noack, Phys. Rev. Lett. **99**, 087203 (2007).
[16] O. Legeza and J. Sólyom, Phys. Rev. B **68**, 195116 (2003).
[17] O. Legeza and J. Sólyom, Phys. Rev. B **70**, 205118 (2004).
[18] T. Giamarchi, *Quantum Physics in One Dimension* (Oxford University Press, New York, 2004).
[19] E. H. Lieb and F. Y. Wu, Phys. Rev. Lett. **20**, 1445 (1968).
[20] P. G. J. van Dongen, Phys. Rev. B **49**, 7904 (1994).
[21] M. Tsuchiizu and A. Furusaki, Phys. Rev. Lett. **88**, 056402 (2002).
[22] M. Nakamura, Phys. Rev. B **61**, 16377 (2000).
[23] P. Sengupta, A. W. Sandvik, and D. K. Campbell, Phys. Rev. B **65**, 155113 (2002).
[24] W. K. Wootters, Phys. Rev. Lett. **80**, 2245 (1998).
[25] L.-A. Wu, M. S. Sarandy, and D. A. Lidar, Phys. Rev. Lett. **93**, 250404 (2004).
[26] R. A. Molina and P. Schmitteckert, Phys. Rev. B **75**, 235104 (2007).
[27] T. J. Osborne and M. A. Nielsen, Phys. Rev. A **66**, 032110 (2002).
[28] A. Osterloh, L. Amico, G. Falci, and R. Fazio, Nature (London) **416**, 608 (2002).
[29] O. F. Syljuåsen, Phys. Rev. A **68**, 060301(R) (2003).
[30] S.-J. Gu, H.-Q. Lin, and Y.-Q. Li, Phys. Rev. A **68**, 042330 (2003).
[31] T. Roscilde, P. Verrucchi, A. Fubini, S. Haas, and V. Tognetti, Phys. Rev. Lett. **93**, 167203 (2004).
[32] J. Preskill, Physics 229: Quantum information and computation (1998), lecture notes (http://www.theory.caltech.edu/~preskill/ph229/#lecture).
[33] G. Vidal and R. F. Werner, Phys. Rev. A **65**, 032314 (2002).
[34] J. Rissler, R. M. Noack, and S. R. White, Chem. Phys. **323**, 519 (2006).
[35] G. Vidal, J. I. Latorre, E. Rico, and A. Kitaev, Phys. Rev. Lett. **90**, 227902 (2003).
[36] N. Laflorencie, E. S. Sørensen, M.-S. Chang, and I. Affleck, Phys. Rev. Lett. **96**, 100603 (2006).